Harmful Algae 129 (2023) 102529

Contents lists available at ScienceDirect

Harmful Algae

journal homepage: www.elsevier.com/locate/hal

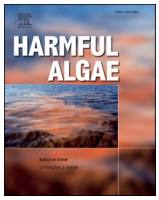

Metabolomics and lipidomics reveal the effects of the toxic dinoflagellate *Alexandrium catenella* on immune cells of the blue mussel, *Mytilus edulis*

Stéphane Beauclercq [a], Olivier Grenier [b], Alexandre A. Arnold [a], Dror E. Warschawski [c], Gary H. Wikfors [d], Bertrand Genard [b,e], Réjean Tremblay [b], Isabelle Marcotte [a,*]

[a] Department of Chemistry, Université du Québec à Montréal, P.O. Box 8888, Downtown Station, Montréal, QC, Canada
[b] Institut des Sciences de la Mer de Rimouski, Université du Québec à Rimouski, Rimouski, QC, Canada
[c] Laboratoire des Biomolécules, LBM, CNRS UMR 7203, Sorbonne Université, École Normale Supérieure, PSL University, Paris, France
[d] Northeast Fisheries Science Center (NEFSC), NOAA Fisheries, Milford, CT, USA
[e] Les laboratoires Iso-BioKem Inc., 367 rue Gratien-Gélinas, Rimouski, QC, Canada

ARTICLE INFO

Edited by: Dr Holly Bowers

Keywords:
Paralytic shellfish poisoning
Harmful algal bloom
Mussel immune cells
Activity assays
NMR-based metabolomics
Lipid composition

ABSTRACT

The increasing occurrence of harmful algal blooms, mostly of the dinoflagellate *Alexandrium catenella* in Canada, profoundly disrupts mussel aquaculture. These filter-feeding shellfish feed on *A. catenella* and accumulate paralytic shellfish toxins, such as saxitoxin, in tissues, making them unsafe for human consumption. Algal toxins also have detrimental effects upon several physiological functions in mussels, but particularly on the activity of hemocytes – the mussel immune cells. The objective of this work was to determine the effects of experimental exposure to *A. catenella* upon hemocyte metabolism and activity in the blue mussel, *Mytilus edulis*. To do so, mussels were exposed to cultures of the toxic dinoflagellate *A. catenella* for 120 h. The resulting mussel saxitoxin load had measurable effects upon survival of hemocytes and induced a stress response measured as increased ROS production. The neutral lipid fraction of mussel hemocytes decreased two-fold, suggesting a differential use of lipids. Metabolomic ^{1}H nuclear magnetic resonance (NMR) analysis showed that *A. catenella* modified the energy metabolism of hemocytes as well as hemocyte osmolyte composition. The modified energy metabolism was reenforced by contrasting plasma metabolomes between control and exposed mussels, suggesting that the blue mussel may reduce feed assimilation when exposed to *A. catenella*.

1. Introduction

Aquaculture production is increasing worldwide in response to strong demand for seafood coupled with flat wild fishery landings (FAO, 2020). The blue mussel, including two species *Mytilus edulis* and *Mytilus trossulus* (Tremblay and Landry, 2016), is an important source of income for Canadian aquaculture as its production volume and value are the largest of all harvested molluscs (Statistics-Canada, 2019). Mussel farming occurs in the natural environment, thus exposing mussels to various environmental risks, including the presence of toxin-producing microalgae or other bioactive compounds during harmful algal blooms (HAB) (Lassudrie et al., 2020), that are expected to increase with climate change (Boivin-Rioux et al., 2021). As filter-feeding organisms, mussels ingest, assimilate, and accumulate HAB toxins in their tissues (Galimany et al., 2008a). These toxins can be harmful to mussels by disrupting several physiological functions, such as feeding activity, sodium-channel mutation, and valve microclosures, in some cases leading to tissue damage, paralysis, altered behavior, and loss of homeostasis (Lavaud et al., 2021; Bianchi et al., 2019; Comeau et al., 2019; Pousse et al., 2019; Tran et al., 2010; Hegaret et al., 2007; Bricelj et al., 2005). Microalgal biotoxins can also affect specific cellular immune-function activities, such as the apoptosis of immune cells or changes in hematology (Galimany et al., 2008a; Hegaret et al., 2007).

The dinoflagellate *Alexandrium catenella*, is recognized as one of the main, recurring HAB species in Canada (Boivin-Rioux et al., 2021; Starr et al., 2017; John et al., 2014; Blasco et al., 2003). Dinoflagellate species responsible for HAB produce a complex mixture of toxins from the family of paralytic shellfish toxins (PSTs), including saxitoxin (STX), neosaxitoxin (nSTX), gonyautoxin (GTX) and other variants of these molecules (Cusick and Sayler, 2013).

Saxitoxin is recognized as a threat to human health when ingested, resulting in potentially fatal illnesses (Wang et al., 2003). The toxicity

* Corresponding author.
E-mail address: marcotte.isabelle@uqam.ca (I. Marcotte).

https://doi.org/10.1016/j.hal.2023.102529
Received 15 May 2023; Received in revised form 13 September 2023; Accepted 16 October 2023
Available online 20 October 2023

limit of STX for safe human consumption of bivalve shellfish is 80 μg equivalent of STX per 100 g of tissue. Distribution and sale of the blue mussel is forbidden above this threshold (Bates et al., 2020). Previous cultures of A. catenella produced at the UQAR aquaculture research station reached toxin cell quotas ranging between 3 and 60 pg STXeq·cell^{-1} (Lavaud et al., 2021). Among the bivalve responses to HAB toxins, those in hemocytes, responsible for innate-immune defense, are the consequence of both the mechanism of HAB effect and the protective response of the mussels. Several studies have revealed biotoxins effects on specific cellular immune-function activities, such as apoptosis of immune cells or changes in hematology (Galimany et al., 2008b).

Hemocytes are specialized bivalve cells involved in digestion, nutrient transport, excretion, detoxification, shell mineralization, tissue repair, and, most importantly, immunity (Gosling, 2008). The immune system of bivalves is exclusively innate and relies upon the circulating hemocytes to act by phagocytosis or encapsulation of infective agents, and subsequent elimination of bacteria, cell debris, protozoa, and potential toxic algae (Cheng, 1996). Blue mussels have been classified as rapid detoxifiers, eliminating toxins within weeks (Lavaud et al., 2021; Nielsen et al., 2016). PSTs at low doses increase the phagocytic activity of hemocytes in mussels, with a moderate incidence of lysosomal damage (Bianchi et al., 2021). This phagocytic activity is thought to modify the hemocyte lipidome and membrane organization (Leroux et al., 2022). Hemocyte membrane changes may affect the immune response of mussels, because the cell membrane is an important participant in hemocyte immune responses. Specifically, arachidonic acid (20:4n6) seems to be vital to maintain cellular activities (le Grand et al., 2011, 2013, 2014; Delaporte et al., 2006), but can be targeted by the production of reactive oxygen species (ROS), another defense mechanism active in hemocytes (Winston et al., 1996) and arising from mitochondria (Donaghy et al., 2012). ROS contain one or more unpaired electrons that have high oxidizing power and rapidly react with compounds having pairs of electrons, such as double bonds in mono- or poly-unsaturated fatty acids (MUFA and PUFA) (Turrens, 2003).

Knowledge of the biochemical pathways in mussel immune cells during HAB exposure is limited. Biochemical studies of immune response to foreign bodies have mostly focused on the hemolymph, the circulatory fluid of bivalves distributing throughout the body containing nutrients, respiratory gases, enzymes, metabolic wastes, and toxicants, as well as hemocytes (Frizzo et al., 2021; Campos et al., 2015). The central role of hemocytes in the immune system makes them ideal to detect biochemical responses of mollusks to HAB or other particles; therefore, we investigated the effect of a conspecific HAB upon mussel immune cells though the application of metabolomics to the hemocytes.

Metabolomics provides high-throughput qualitative and quantitative analyses of metabolites within cells, tissues, or biofluids. Techniques based upon mass spectrometry (MS) or nuclear magnetic resonance spectroscopy (NMR) data have been used extensively in biomedical science, and more recently in the fields of aquaculture and marine ecology (Bayona et al., 2022; Nguyen and Alfaro, 2020; Young and Alfaro, 2018). Most of these studies have been conducted using MS, and fewer studies were conducted by NMR spectroscopy, despite its ease of implementation (Frizzo et al., 2021; Digilio et al., 2016). Proton (^{1}H) NMR-based metabolomics was chosen to characterize any biochemical changes in *M. edulis* hemocytes exposed to *A. catenella*. Furthermore, hemocyte membrane lipid composition was investigated for its importance in the phagocytic process. Finally, the effects of a HAB upon *M. edulis* general metabolism were characterized through NMR analysis of the plasma separated from the hemocytes. To the best of our knowledge, this study is the first to apply metabolomics profiling to bivalve hemocytes.

2. Materials and methods

2.1. Experimental mussel collection

Mytilus edulis mussels [length 57.8 (3.7) mm] were sampled in two batches of 120 individuals each, from aquaculture farm long lines in Malpeque Bay (Prince Edward Island, Canada, 46.54024 N, −63.80926 W), and transported to the wet laboratory research facilities of the Université du Québec à Rimouski (Pointe-au-Père, QC, Canada). Mussels were scrubbed, rinsed with UV-treated, filtered (1 μm) seawater and acclimated for 30 days in two 100 L open-flow tanks with a gradual increase in temperature for the first 10 days of ~1 °C per day until reaching 20 °C. During this period, mussels were fed a diet composed of mass-cultured *Tetraselmis suecica* CCMP 904, *Tisochrysis lutea* CCMP 1324, *Chaetoceros muelleri*, CCMP 1316, and *Diacronema lutheri* CCMP 1325 (1:1:1) at a rate of 4×10^7 cells indiv^{-1}day^{-1} (equivalent to 1% of dry weight per day). Algal strains were obtained from the Provasoli-Guillard National Center for Marine Algae and Microbiota (NCMA, Maine, USA) and cultured in autoclaved 20 L bottles with F/2-Si nutrient enrichment, daylight 24/0 (D/N) at light intensity of 100 μm m^{-2}s^{-1} PAR at 20 °C.

An *Alexandrium catenella* isolate (clone named AC6, Lavaud et al., 2021) was obtained from the St. Lawrence Estuary (Canada) during a bloom monitored in 2008 (Starr et al., 2017) and grown under the same axenic conditions as the nontoxic microalgae, generating toxin cell quotas between 3 and 60 pg STXeq·cell^{-1} (Lavaud et al., 2021).

2.2. Exposure of mussels to cultured Alexandrium catenella

Mussels from each batch were brushed with diluted hypochloric acid (<1 %), rinsed with UV-treated, filtered (1 μm) seawater, and distributed into eight 30 L conical-bottom tanks (15 mussels per tank) filled with UV-treated, 0.1 μm-filtered seawater at 20 °C with food addition similar to that of the acclimation period. A volume representing 50 % of the seawater in each tank was changed daily. During the 120 h of the experiment, mussels in four tanks were fed *A. catenella* daily by peristaltic pumps at a concentration of 182 cells mL^{-1} (equivalent to 3.6×10^5 cells ind^{-1}d^{-1} or 1 % of their dry weight) in addition to the acclimation diet. In the control treatment, mussels in four other tanks were supplemented with 520 cells mL^{-1} per day of cultured *Tetraselmis suecica* (in addition to the acclimation diet), to obtain similar microalgal biomass in both treatments. During the experimental period, no mussel mortality or spawning event was observed.

2.3. Hemocyte sampling

After 120 h of exposure to toxic algae, mussels were sampled in each tank. The hemolymph (0.5 to 1 mL) was collected from the pericardial cavity/adductor muscle sinus with a sterile, 21 G gauge needle using a 1 mL syringe. Hemolymph samples were filtered through an 80 μm mesh and stored in Eppendorf microcentrifuge tubes held on ice, for cell activity analyses and hemocyte morphology of individual mussels with the first batch, and for solution NMR-based metabolomics with the second batch. No intermediate sampling of hemolymph was perform to be able to collect enough hemocyte for the NMR measurements after the 120 h of exposure to *A. catenella*.

For solution NMR analysis, the hemolymph was combined into six pools from 10 mussels randomly collected among the 60 mussels in the four tanks for each treatment, in 15 mL conical-bottom centrifuge tubes kept on ice, and immediately centrifuged at 800 × g at 4 °C for 15 min to separate the hemocytes from the plasma (Frizzo et al., 2021). Hemocyte recovery was 100 to 200 mg from the hemolymph in each pool. The pelleted hemocytes and plasma fractions were transferred into new 15 mL, conical-bottom centrifuge tubes and frozen immediately at −80 °C until metabolite extraction.

For lipid composition analysis of the first batch, the remaining

hemolymph and hemocytes were randomly pooled together into three samples (20 mussels/sample) per treatment, centrifuged (8000 × g, for 5 min at 4 °C), and the supernatant was partially removed. The hemocytes were rinsed 5 times with 0.2 μm-filtered seawater and centrifuged under the same conditions for 2 min. The 6 samples of purified hemocytes were then placed in 2 mL amber glass vials with Teflon-lined caps.

2.4. Cell activity analyses

Procedures for characterization of the hemocytes, granular/agranular subpopulations, hemocyte mortality, state of apoptosis of dead or living cells, percentage of apoptotic cells, and unstimulated hemocyte production of ROS were adapted from previous studies (Donaghy et al., 2012; Galimany et al., 2008b; Soudant et al., 2004; Hegaret et al., 2003). The hemocytes and plasmas were extracted from the six pools of hemolymph for each treatment, as described above. Hemocyte counting was carried out using a BD Accuri™ C6 flow cytometer (BD Biosciences, San Jose, CA, USA). The detection method used for the hemocytes involved staining one subsample with SYBR Green (a DNA-binding probe which spontaneously penetrates both viable and dead cells) to detect all hemocytes, and propidium iodide (PI) to detect dead cells. To differentiate cells undergoing apoptosis, another subsample was stained with both PI and AnnexinV, which is a membrane inversion marker, an early step in programmed cell death (PCD). This method allows the detection of four cell types in a single assay: non-apoptotic living cells, apoptotic living cells (the membrane has inverted as an early step in PCD but the membrane remains impermeable to PI), apoptotic dead cells (permeable to PI and membrane has inverted), and non-apoptotic dead cells (permeable to PI and membrane has not inverted, cells have died by necrosis).

M. edulis hemocytes are composed of two subpopulations, agranulocytes and granulocytes, whose morphology was determined based upon flow-cytometric parameters, Forward Scatter (FSC) and Side Scatter (SSC), as described in Donaghy et al. (2012). FSC and SSC commonly measure particle size and internal complexity, respectively.

Determination of ROS production was performed using 2′7′-dichlorofluorescein diacetate (DCFH-DA; Molecular Probes, Invitrogen), at a final concentration of 10 μM, a membrane permeable and non-fluorescent probe as described in Donaghy et al. (2012). Inside hemocytes, the -DA radical is hydrolyzed by esterase enzymes. DCFH is oxidized by intracellular hydrogen peroxide (H_2O_2) and superoxide ion to the fluorescent DCF molecule. DCF green fluorescence was detected on the FL1 detector (530/30 nm band pass) of the flow cytometer, and it is proportional to cellular ROS production. Relative ROS production is expressed as DCF fluorescence in arbitrary units (AU).

2.5. Lipid composition

Hemocytes were pooled into three samples per treatment, as described above, and lipids were extracted by grinding the hemocyte samples in dichloromethane–methanol using a modified Folch procedure as described in Parrish (1999). The lipid content and class composition were determined using a flame-ionization detection system (Parrish, 1987), with silica-gel-coated chromarods (S-V Chromarods; Shell-USA). Each lipid extract was scanned by an Iatroscan (Mark-VI, Iatron Laboratories) to separate aliphatic wax esters, ketones, triacylglycerols, alcohols, sterols, acetone mobile polar lipids, and phospholipids. For each lipid class, standards were used (Sigma Aldrich, Oakville, ON, Canada). Chromatograms were analyzed using the integration software Peak Simple version 3.2 (SRI). Total lipids (expressed as μg mg^{-1}) are the sum of all classes, and each class is expressed as relative concentration (% of total lipids).

Lipid extracts were separated into neutral and polar fractions by column chromatography on silica-gel micro-columns (30 × 5 mm i.d., packed with Kieselgel 60, 70–230 μm mesh; Merck, Darmstadt, Germany) using chloroform:methanol (98:2, v/v) to elute neutral lipids, followed by methanol to elute polar lipids (Marty et al., 1992). Fatty-acid profiles of polar lipids were determined on fatty-acid methyl esters (FAMEs) using sulfuric acid:methanol (2:98, v:v) and toluene. FAMEs of neutral and polar fractions were concentrated in hexane, and the neutral fraction was purified on an activated silica gel with 1 mL of hexane:ethyl acetate (v/v) to eliminate free sterols. FAMEs were analysed in the full scan mode (ionic range: 50–650 *m/z*) on a Polaris Q ion-trap-coupled multichannel gas chromatograph "Trace GC ultra" (Thermo Scientific, MA, USA) equipped with an autosampler model Triplus, a PTV injector, and a mass detector model ITQ900 (Thermo Scientific, MA, USA). The separation was performed with an Omegawax 250 (Supelco) capillary column with high purity helium as the carrier gas. Data were treated using Xcalibur v.2.1 software (Thermo Scientific, MA, USA). Tricosanoic acid (23:0) was employed as an internal standard. FAMEs were identified and quantified using known standards (Supelco 37 Component FAME Mix and menhaden oil; Supleco), and were further confirmed by MS.

2.6. Hemocyte and plasma extraction for solution NMR

Metabolites were extracted from the 6 pools of hemocytes from 10 mussels per treatment, using an adaptation of Folch's method (Madji Hounoum et al., 2015). Briefly, 3 mL of ice-cold methanol followed by 3 mL of dichloromethane were added to the conical centrifuge tubes containing the hemocytes previously thawed on ice. The mixtures were vortexed for 1 min and sonicated (Cole-Parmer Ultrasonic cleaner 08892, Vernon Hills, IL, USA) on ice for 10 min before addition of 2 mL cold, extra-pure water and 30 s agitation. Following cooling at −20 °C for 40 min to precipitate proteins, the samples were centrifuged at 7100 × g at 4 °C for 15 min to separate the polar and lipidic fractions. The polar fractions were collected in glass tubes, and the solvent was evaporated in a SpeedVac (Thermo Fisher Scientific, Waltham, MA, USA) at room temperature. Plasma samples for ^{1}H NMR were prepared by cold methanol precipitation of lipids and proteins (Beauclercq et al., 2016). Briefly, 500 μL of unfrozen plasma samples were mixed with 1 mL of ice-cold methanol and cooled at −20 °C for 20 min. The mixes were then centrifuged at 15,000 × g at 4 °C for 10 min, and the supernatants were collected in microtubes for further solvent evaporation in a SpeedVac at room temperature.

2.7. Solution NMR-based metabolomics

2.7.1. NMR spectroscopy measurements

Prior to NMR analysis, hemocyte extracts and plasma samples were reconstituted in 500 μL of 0.2 M pH 7.4 potassium phosphate buffer in 99.9 % deuterium oxide (D_2O) with 0.13 mM 3-trimethylsilylpropionic acid (TSP) as the internal standard. Mixtures were briefly vortexed and centrifuged at 2000 × g for 30 s to remove insoluble components. The resulting supernatants were transferred to 5 mm NMR tubes for analysis.

The ^{1}H NMR spectra from the hemocyte extracts and plasma samples were obtained with a Bruker Avance III spectrometer (Billerica, MA, USA), operating at 600 MHz, with a broad-band inverse TXI probe. NMR measurements were performed at 298 K. The spectra were acquired using a 1D NOESY pulse sequence with a repetition delay of 10 s and mixing time of 50 ms. Water suppression was achieved by presaturation during the repetition delay and mixing time. ^{1}H spectra were collected with 1024 or 256 scans (and eight dummy scans) for the hemocyte extracts or plasma, respectively, in 64k data points with a spectral width of 12 ppm. Spectral data were deposited under the DOI 10.5281/zenodo.7415126 in the Zenodo repository (https://zenodo.org) hosted by the European Organization for Nuclear Research (CERN).

2.7.2. NMR spectra post-processing

Spectra were processed using NMRProcFlow tools (Jacob et al., 2017). The free induction decays (FIDs) were zero-filled to 128k data points, a line-broadening factor of 0.3 Hz was applied prior to Fourier

transformation, and the TSP reference signal was set to 0 ppm. NMR spectra were further processed for peak alignment with NMRProcFlow to minimize spectral peak shift caused by differences in ionic strength within samples. The hemocyte extracts and plasma spectra were then bucketed manually and integrated into 97 and 138 spectral regions (corresponding to one or several metabolites), respectively. The signals from water and methanol were excluded, and the data were normalized by the total sum of all the spectral features, which assumes that only small amounts of metabolites are regulated in approximately equal shares up and down, while all others remain constant (Zacharias et al., 2018). The generated data tables for the hemocyte extracts and plasma were used for multivariate statistical analyses.

2.7.3. Spectral assignment

The identification of metabolites was performed using Chenomx software (Edmonton, Canada), HMDB https://hmdb.ca/ (Wishart et al., 2022), and reference publications on mollusc NMR-based metabolomics (Frizzo et al., 2021; Aru et al., 2020). The annotations of the spectra were further confirmed by 2D ^{1}H NMR COZY and TOCSY experiments performed on a representative sample. The acquisition parameters for those two experiments are provided in Table S1.

2.8. Mussel weight, volume and toxin concentration

At the end of the experiments, soft tissues of each mussel were individually lyophilized to measure the dry mass and estimate the condition index (CI, in g/mm^3) as the ratio of tissue dry weight (DWtissue, g) over volume (V, mm^3). The latter was estimated from the measurement of shell length, width and height with a digital caliper (Mitutoyo 500-196-30 AOS absolute; precision of 0.01 mm). As all the blood was used for flow cytometry and NMR measurement, the amount of saxitoxin was estimated in the whole tissue of each mussel by MS, using a Triple Quad (6420 Agilent Technologies) and Poroshell 120 column (HILIC-Z, 2.1 × 100 mm, 3 μm), with a certified standard from the National Research Council Canada (NRC CRM-STX-g, MRC, Halifax, NS, Canada). The saxitoxin dosage protocol is detailed in the supplementary file.

2.9. Statistical analyses

Values for each hemocyte characteristic and mussel condition index for exposed and non-exposed (control) mussels were compared by Student's *t*-test, following validation of normality and homoscedasticity using the Shapiro–Wilk test. Additionally, linear regression analyses were used between each hemocyte characteristics and saxitoxin concentration in mussel tissues to estimate possible relationships between toxins and hemocyte activities. Standard deviations are indicated in plot brackets.

For the lipid composition of hemocytes, as individual samples were pooled, the replication level corresponded to the tanks (3 for control and 3 for toxic treatment). A distance-based permutational multivariate analysis of variance (PERMANOVA) was used to compare multivariate variables (lipid classes and FA profiles) following assumptions of homoscedasticity verified with the PERMDISP test. *A posteriori* comparisons were done using a PERMANOVA pairwise test. To analyze the similarity between the profiles, non-metric, multi-dimensional scaling (nMDS) and SIMPER analyses were performed, using Euclidian distances. These statistical analyses were done using PRIMER 7.0.21. The significance of the difference between groups was further evaluated through Welch's *t*-test.

An orthogonal projection latent structures discriminant analyses (OPLS-DA) was performed using the Umetrics SIMCA 17 software (Sartorius Stedim, Göttingen, Germany) on hemocyte extracts and plasma ^{1}H NMR data sets. All data were scaled to units of variance. The minimum number of features needed for optimal classification of the OPLS-DA models was determined by iteratively excluding the variables with low regression coefficients and wide confidence intervals derived from jackknifing combined with low variable importance in the projection (VIP) until maximum improvement of the quality of the models (Beauclercq et al., 2022). The model quality was evaluated after 7-fold cross validation by cumulative R^2Y (goodness of fit), cumulative Q^2 (goodness of prediction) and CV-ANOVA (test of cross-validated predictive residuals to assess the reliability of OPLS models). The contribution of each predictor in the model was evaluated through the variable score contribution, *i.e.*, the differences, in scaled units, for all the terms in the model, between the outlying and the normal observation, multiplied by the absolute value of the normalized weight.

3. Results

3.1. Mussel condition index and hemocyte count

To monitor the effect on the blue mussels of a 120 h exposure to *A. catenella*, we determined the condition index, *i.e.,* the relationship between body dry weight and shell length. We also performed a hemocyte count. First, we measured the soft-tissue concentrations of saxitoxin following exposure and hemolymph sampling, which ranged from 3 to 95 μg STX/100 g, with a mean of 26 (22) μg STX/100 g of mussels. At the end of the exposure, no significant difference ($p = 0.08$) in condition index was observed between exposed mussels [13.0 (2.5) g/mm^3] and the control [11.6 (2.1) g/mm^3]. Also, the hemocyte count was similar for the exposed [2258 (2108)] and control mussels [1727 (866), $p = 0.25$].

3.2. Apoptotic activity and ROS production

We also evaluated hemocyte apoptotic activity and ROS production, by flow cytometry with four different probes for possible changes associated with exposure to *A. catenella*. As shown in Table 1, exposure to toxic dinoflagellates modified hemocyte activity, including four major variables related to apoptosis. Specifically, when mussels were exposed to *A. catenella*, the percentage of apoptotic dead cells ($p = 0.009$), non-apoptotic dead cells ($p = 3.95 \times 10^{-7}$) and apoptotic living cells ($p = 1.10 \times 10^{-3}$) decreased, but the mean percentage of non-apoptotic living cells was significantly higher ($p = 2.77 \times 10^{-5}$) as

Table 1
Hemocyte apoptotic status variables determined by flow cytometry for control mussels and mussels exposed (120 h) to *A. catenella*. Variables are presented as [mean (standard deviation)] and with statistical t-Tests on the means differences. Differences with statistical significance ($p \leq 0.05$) are highlighted with bold characters, and the directions of the variations are indicated by arrows.

	Control	Exposed	*t*-test
% non-apoptotic living cells	**61.0 (14.7)**	**↑ 84.7 (20.0)**	**2.77×10^{-5}**
% non-apoptotic dead cells	**29.0 (11.9)**	**↓ 10.6 (12.8)**	**3.95×10^{-7}**
% apoptotic living cells	**2.4 (2.6)**	**↓ 0.8 (1.4)**	**1.10×10^{-3}**
% apoptotic dead cells	**7.7 (8.0)**	**↓ 3.9 (9.1)**	**8.90×10^{-3}**
Agranulocyte complex. (AU)	$2.7\ (0.1) \times 10^{4}$	$2.7\ (0.2) \times 10^{4}$	0.36
Granulocyte complex. (AU)	**$2.9\ (0.3) \times 10^{5}$**	**↓ $2.7\ (0.5) \times 10^{5}$**	**0.05**
Size agranulocyte (AU)	$6.2\ (0.2) \times 10^{5}$	$6.2\ (0.2) \times 10^{5}$	0.29
Size granulocyte (AU)	$2.2\ (0.2) \times 10^{6}$	$2.2\ (0.2) \times 10^{6}$	0.78
% alive agranulocytes	49.1 (13.1)	45.1 (9.5)	0.22
% alive granulocytes	19.4 (6.9)	19.6 (5.1)	0.80
% dead agranulocytes	**14.4 (2.5)**	**↑ 16.2 (2.9)**	**0.04**
% dead granulocytes	17.2 (6.2)	19.2 (5.8)	0.24
ROS agranular cells (AU)	**2306 (416)**	**↑ 3622 (1612)**	**5.27×10^{-6}**
ROS granular cells (AU)	73,017 (44,002)	81,618 (52,059)	0.19

compared to the control. There were no significant correlations between hemocyte apoptotic-associated variables and the saxitoxin concentration measured in the whole mussel tissues (Table S2). Thus, regardless of the concentration of saxitoxin, most cells remained alive and non-apoptotic in mussels exposed to *A. catenella*.

Two subpopulations of hemocytes differing in size and granularity were identified, *i.e.,* the granulocytes and agranulocytes. The granulocytes, which contain granules, were larger than the agranulocytes and accounted for ~40 % of all hemocytes (Table 1). Although the majority of granulocytes and agranulocytes were alive in both treatments, the exposure to *A. catenella* induced a higher mortality percentage in the agranulocyte population ($p = 0.035$) as well as a 1.6-time rise in ROS production ($p = 5.27 \times 10^{-6}$). Moreover, the complexity, or granularity, of the granulocytes, was significantly higher in the "toxic" treatment ($p = 0.05$).

3.3. Lipid composition of hemocyte membranes

Lipid composition analysis of the hemocyte membranes revealed differences between the polar and neutral fractions (DF = 1 and 11, Pseudo-$F = 6249$, $p = 0.0001$). Indeed, the polar fraction showed the presence of 56 % phospholipids and the absence of triglycerides; whereas, the neutral fraction contained 55 % triglycerides and no phospholipids. Simper analysis indicated that these two lipid classes explain more than 83 % of the dissimilarity between the polar and neutral lipid profiles. Both hemocyte lipid fractions had similar lipid class composition, whether exposed or not to *A. catenella* (Fig. 1). Total lipids, however, represented by the sum of the concentration of each lipid class, showed significant interactions between lipid fractions (neutral and polar) and conditions (DF = 1 and 11, Pseudo-$F = 13$, $p = 0.0064$). Differences attributable to the toxic exposure were not observed in the polar fraction, in contrast to the neutral fraction in toxin-exposed mussels, which showed less than half the lipid concentration ($p = 0.0092$) of the control [300 (50) *vs.* 650 (130) mg g^{-1} dry mass].

The fatty acid (FA) profiles of the lipid fractions from the hemocytes of mussels exposed to the PST-producing dinoflagellate and from those exposed to the forage *T. suecica* algae were different (Fig. 2). A significant interaction was observed (DF = 1 and 11, Pseudo-$F = 5.25$, $p = 0.0108$), and associated with differences in the FAs profile only in the polar fraction ($p = 0.0049$), but not in the neutral fraction ($p = 0.8365$). The Simper analysis indicates that these are related to the saturated FAs 16:0 (19.3 %) and 18:0 (9.4 %), with relative abundances higher in the control ($p = 0.004$), as well as the unsaturated FAs 20:5n3 (29.5 %), 20:4n6 (9.7 %), 20:1n9 (8.9 %), 22:6n3 (8.2 %) in higher abundance in the toxic group (Fig. 3). The differences between groups were significant ($p \leq 0.05$) for C16:0, C18:0, C20:1n9, and C22:6n3.

3.4. Hemocyte and plasma metabolomes by solution NMR

Annotated representative ^{1}H NMR spectra of the hemocyte extracts and of the plasma are shown in Fig. 4. The NMR spectra were divided into 97 and 138 buckets corresponding to 59 and 55 identified metabolites for the hemocyte extracts and the plasma samples, respectively. The percentage of unidentified buckets were 17 % in the spectra of the hemocyte extracts and 15 % in the plasma samples. The identified metabolites belonged mainly to 5 classes: amino acids, FAs and conjugated, purines, pyrimidines, and tricarboxylic acid cycle (TAC) acids.

OPLS-DA models were adjusted to the metabolome of the hemocytes and plasma of mussels exposed or not to *A. catenella* to explore possible effects of the toxic dinoflagellate upon the immune system and general metabolism of the mussels. The first model was fitted to the hemocyte metabolomics data and contained a subset of 35 buckets corresponding to 28 identified metabolites (Fig. 5). The model was composed of one predictive and one orthogonal component with an explicative ability (R^2Y) of 0.94 and a predictive ability (Q^2) of 0.71 (CV-ANOVA = 0.05). The metabolites included in the models belonged mainly to the classes of amino acids, purines, and pyrimidines. Purines such as adenosine monophosphate (AMP), adenosine diphosphate (ADP), and guanosine monophosphate (GMP), amines (dimethylamine), carboxylic acids (formate), and some amino acids (dimethylglycine, glycine, phenylalanine, isoleucine, lysine, aspartic acid, sarcosine, arginine) were more plentiful in the hemocytes after toxic treatment. On the other hand, alanine, serine, tyrosine and the purine adenosine triphosphate (ATP) as well as pyrimidines (uridine monophosphate (UMP), uridine

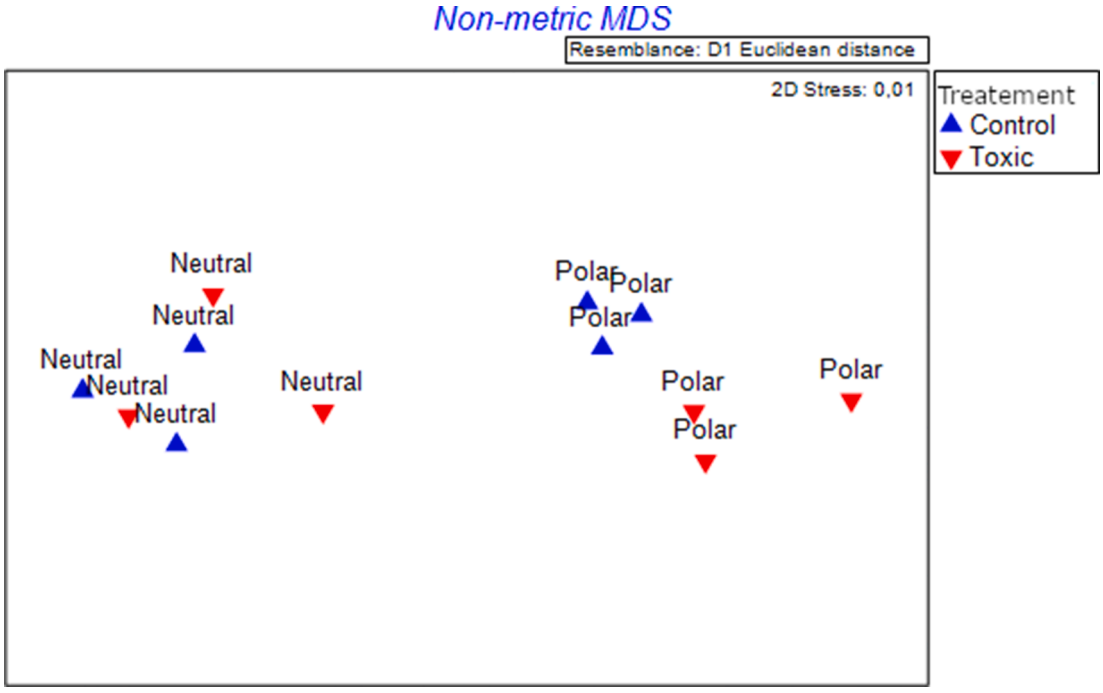

Fig. 1. Non-metric multi-dimensional scaling of the Euclidian similarity matrix based on the relative abundance of lipids classes in the neutral and polar lipid fractions of hemocytes exposed (Toxic, blue) or not (Control, red) to *A. catenella*.

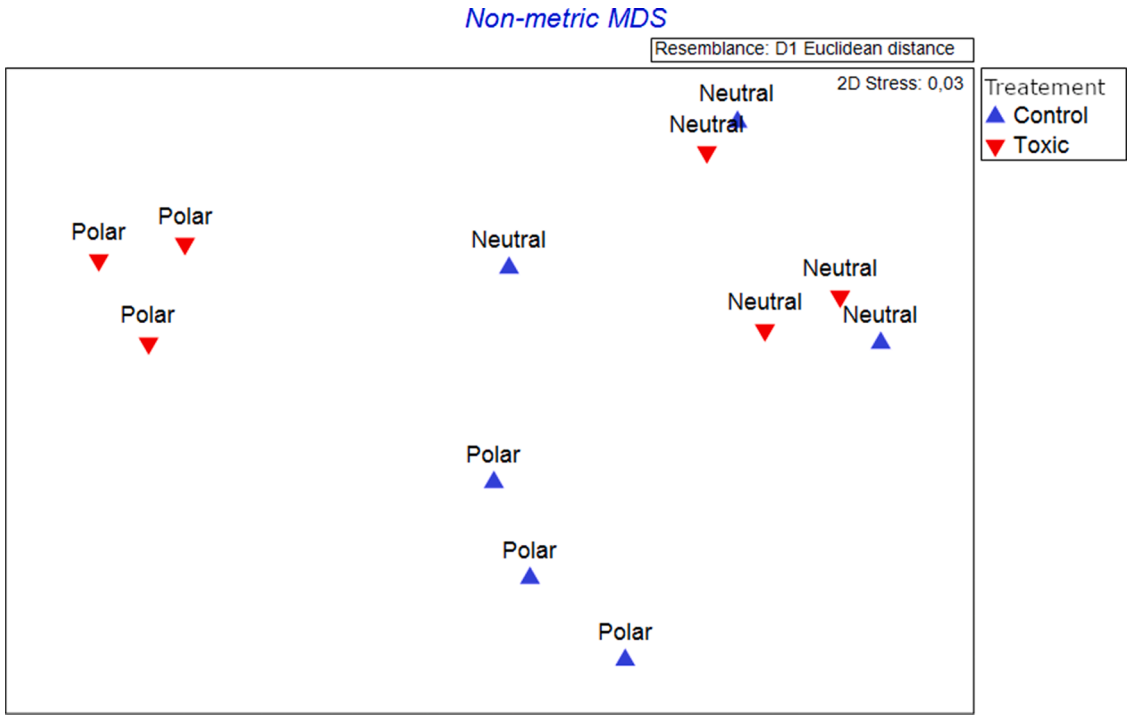

Fig. 2. Non-metric multi-dimensional scaling of the Euclidian similarity matrix based on the relative abundance of fatty acids in the neutral and polar lipid fractions of hemocytes exposed (Toxic, red) or not (Control, blue) to *A. catenella*.

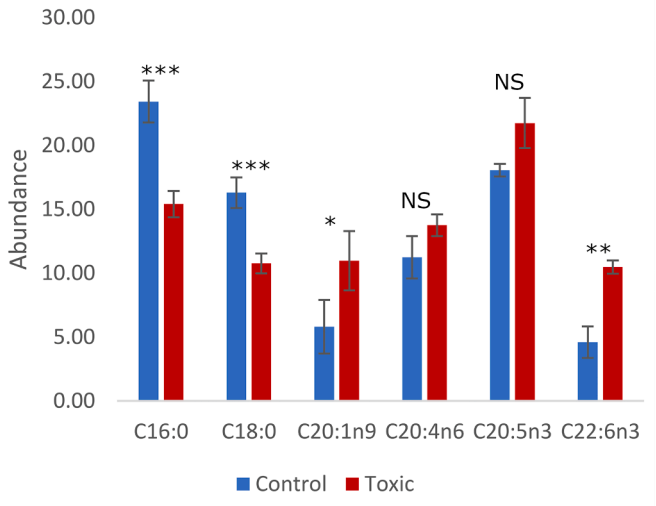

Fig. 3. Relative abundances of the six fatty acids in the polar lipid fraction that contributed to 85 % of the differences between hemocytes exposed (Toxic, red) or not (Control, blue) to *A. catenella* in Simper analysis. The significance of the differences between groups was further evaluated through Welch's *t*-test (*P*-value NS > 0.05, * ≤ 0.05, ** ≤ 0.01, *** ≤ 0.005).

diphosphate UDP/UDP-glucose, uracil), sulfonic acids (taurine), disaccharides (maltose), alkaloids (trigonelline), monosaccharides (glucose), benzamides (mytilitol), and fatty esters (acetylcarnitine) were lower in the hemocyte extracts of mussels exposed to the toxic treatment.

The second OPLS-DA model based on plasma data aimed to assess the effects of an exposure to *A. catenella* on the global metabolism of the mussels (Fig. 6). This model was composed of 32 buckets projected to one predictive and one orthogonal components with a R^2Y of 0.92 and a Q^2 of 0.78 (CV-ANOVA = 0.02). As for the hemocytes, the 25 metabolites in the model were mostly amino acids, purines, and pyrimidines. Amino acids (dimethylglycine, Glu, Tyr, Phe, Ala, Ser, Asp, Ornithine, Arg, Gln, Trp), pyrimidines (UDP, uracil), disaccharides (maltose), alkaloids (trigonelline), monosaccharides (glucose), benzamides (mytilitol), carboxylic acid (glycolate), and sulfonic acid (hypotaurine) were higher in the control condition. Conversely, the purines AMP and ADP, sulfonic acid taurine, amino acids betaine and homarine, as well as FAs and conjugates (2-aminobutyrate) were markers of *A. catenella* exposure.

4. Discussion

In this work, we assessed some effects of a 120 h exposure of *M. edulis* to *A. catenella*. We determined a mean concentration in whole mussel soft tissues of 26 (23) µg STX/100 g saxitoxin in the soft tissue, *i.e.*, below the threshold of 80 µg STXeq/100 g at which blue mussels are considered inedible (Bates et al., 2020). Nevertheless, significant effects were detected upon hemocyte activity, lipid composition, and metabolome, as well as mussel general metabolism as determined by the plasma metabolome.

4.1. Immune cell responses to A. catenella exposure

Our results showed that the percentage of live hemocytes in circulation was slightly higher following exposure to *A. catenella* as compared to the control group, despite possible lethal effects of toxins upon mussels, as reported by Bianchi et al. (2021). The moderate levels of toxins accumulated in mussels and short exposure time could explain this result. Hemocytes in exposed mussels were not going through the normal cellular death cycle because the production and use of hemocytes was necessary to respond to the toxic dinoflagellate by encapsulating and expelling them in the alimentary canal (Hegaret et al., 2007). Granulocytes are the most active phagocytic cells (Wikfors and Alix, 2014) and have a higher ability to produce ROS (de la Ballina et al., 2022). Our results showed that the granularity of the granulocytes was increased following toxic-algal treatment, which could be related to the internalization of algal toxins and detoxification through enzymatic

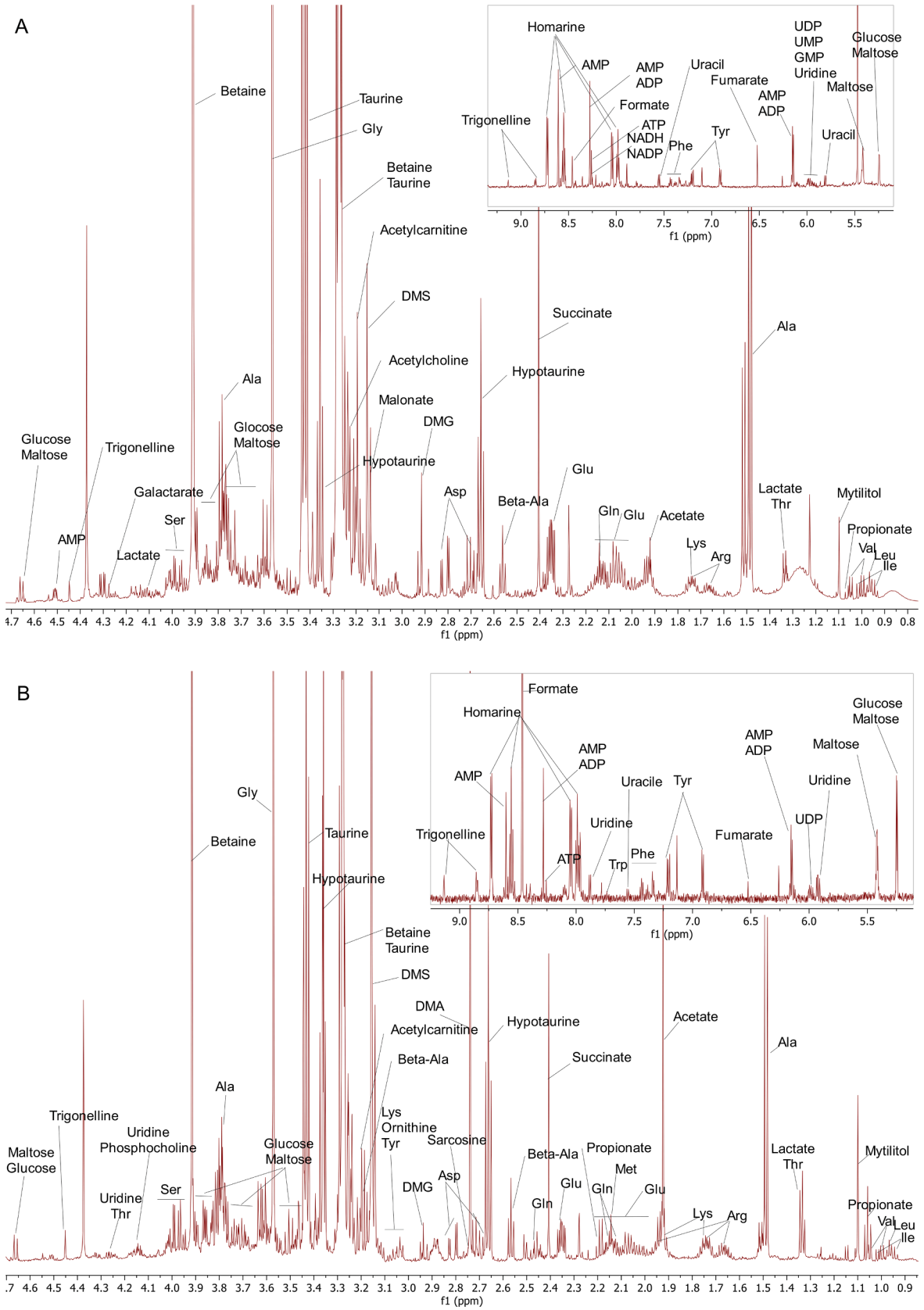

Fig. 4. Representative annotated ^{1}H NMR spectra of (A) the hemocyte extract and (B) plasma. DMA: dimethylamine, DMG: dimethylglycine, DMS: dimethyl sulfone.

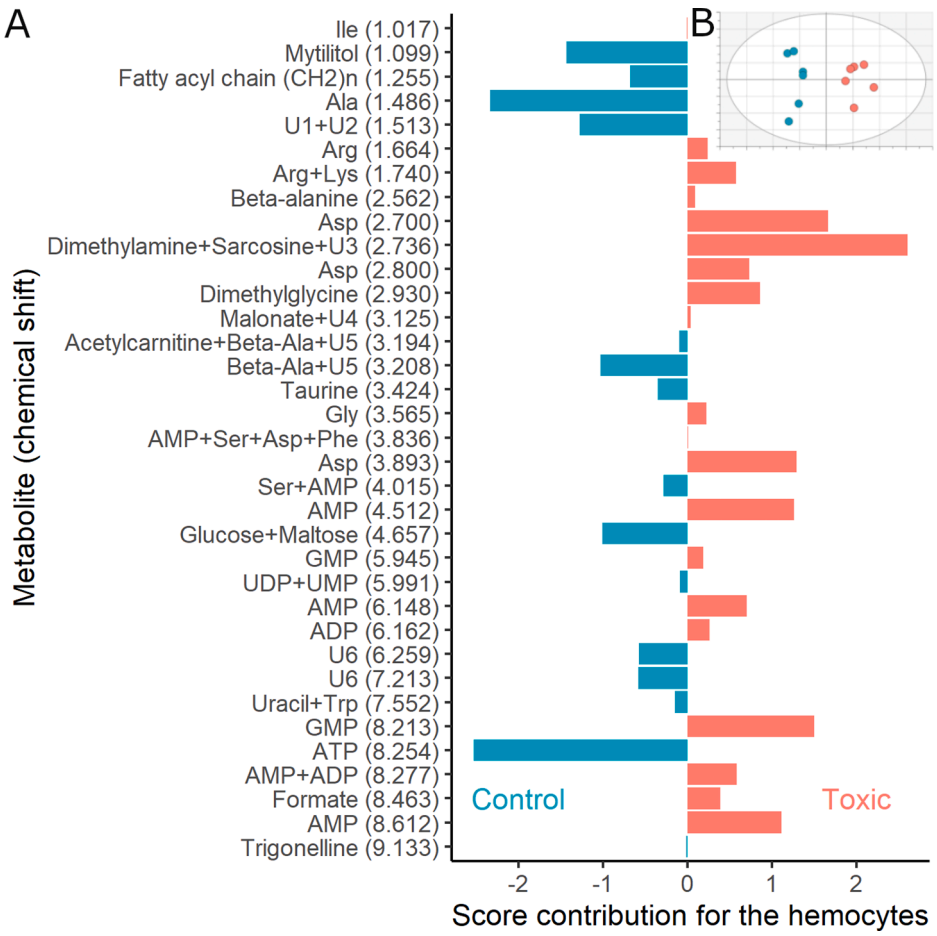

Fig. 5. Metabolomic analysis of the effect on the hemocytes of a 120 h exposure to *A. catenella*. (A) Contributions plot, indicative of the contribution of hemocyte metabolites identified in the OPLS-DA. (B) Score plot following OPLS-DA with the treatment as categorical factor Y and the metabolites as explanatory qualitative variables X. The hemocyte samples exposed to *A. catenella* and the control are represented by pink and turquoise circles, respectively. The model contained 35 buckets, 1 predictive and 1 orthogonal components, and its descriptive and predictive performance were $R^2Y = 0.94$ and $Q^2 = 0.71$.

activities. However, further analysis, such as measuring phagocyte activity of the hemocytes could confirm this hypothesis. Active detoxification and elimination of toxin metabolites by diapedesis of hemocytes into the mussel gut (Galimany et al., 2008b) would leave fewer hemocytes cycling through apoptosis.

Conversely, the mortality of the agranulocytes was higher in the toxic treatment, suggesting that these cells are more vulnerable to microalgal toxins than the immuno-competent granular cells, as was observed for Pacific oyster *Crassostrea gigas* hemocytes exposed to saxitoxin (Abi-Khalil et al., 2017). Moreover, the ROS production by the agranulocytes from the STX-exposed mussels was higher, indicating a generalized stress response. It has been demonstrated that both hemocyte subpopulations contribute to the production of ROS, with the granulocytes being the most active cells (Andreyeva et al., 2019). Intracellular ROS increase in agranulocytes, as observed in our study, is seen in hypoxic conditions, consistent with the increased oxygen consumption rate previously recorded during exposure of mussels to *A. catenella* (Lavaud et al., 2021). Meanwhile, the production of ROS remained stable in granulocytes, as the intracellular ROS production is part of the detoxification, defense response (Bianchi et al., 2021). Thus, moderate levels of toxins may have an indirect effect upon the production of ROS in the agranulocytes, through the increase of oxygen consumption associated with stress.

4.2. Modification of hemocyte neutral lipid composition

Exposing molluscs to harmful substances can affect the lipid composition of hemocytes (Leroux et al., 2022). *A. catenella* is no exception; our results showed that STX-exposed mussels responded with a decrease in hemocyte neutral lipids (triacylglycerides (TAGs), ketones, sterols, acetone mobile polar lipids) in comparison to the control. A study of *M. galloprovincialis* hemocytes exposed to nanoplastics showed that TAGs were the most abundant class of lipids released into the culture medium, suggesting increased release of TAG-enriched vesicles (Leroux et al., 2022). Similarly, the lower concentration of neutral lipids in the hemocytes after exposure to *A. catenella* could be attributable to a preferential use in excretion vesicles containing the algal toxins or participation in ROS oxidative consumption. Some neutral lipids such as TAGs can also be used in the production of energy (Cantrell and Mohiuddin, 2022). Indeed, immune stimulation is an energy-demanding process, therefore TAGs and phospholipids could be hydrolyzed by the hepatic lipases in the digestive gland to provide free FAs to maintain energy requirements, thereby limiting availability for the production of hemocytes (Qiu et al., 2020).

The FA composition was different between treatments only in the polar fraction. Two saturated FA (palmitic acid [16:0] and stearic acid [18:0]), one monounsaturated FA (MUFA) (eicosenoic acid [20:1n9]) and three polyunsaturated FAs (PUFA) (arachidonic acid [20:4n6], eicosapentaenoic acid [20:5n3], docohexaenoic acid [22:6n3]) were the major contributors to this difference (85 %). More specifically, the two saturated FAs were more concentrated in the control, while the MUFAs and PUFAs were more concentrated in the STX-exposed hemocytes. This result suggest that hemocyte membrane lipids did not participate in the oxidation processes following increased ROS production induced by the

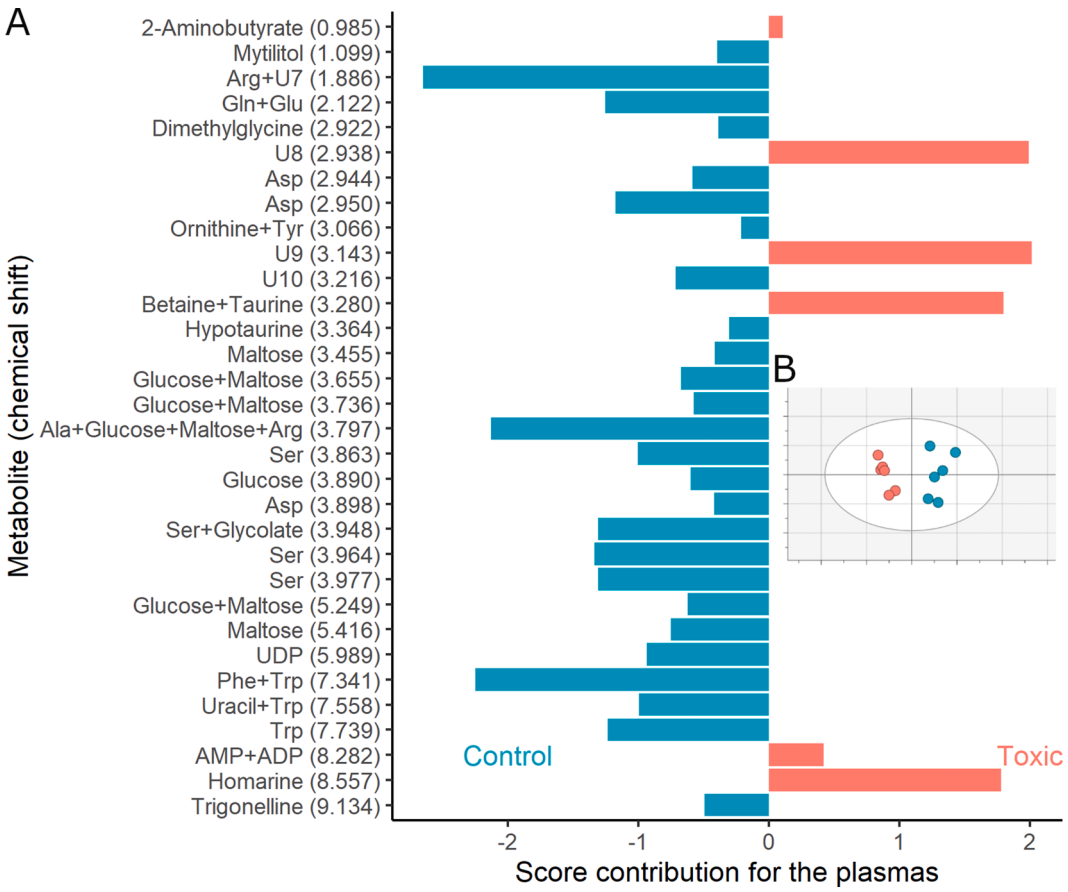

Fig. 6. Metabolomic analysis of the effect on the plasma of a 120 h exposure to *A. catenella*. (A) Contributions plot indicative of the contribution of plasma metabolites identified in the OPLS-DA. (B) Score plot following OPLS-DA. The plasma samples exposed to *A. catenella* and the control are represented by pink and turquoise circles, respectively. The model contained 32 buckets, 1 predictive and 1 orthogonal components, and its descriptive and predictive performance were $R^2Y = 0.92$ and $Q^2 = 0.78$.

A. catenella treatment, which usually reduces by peroxidation the amount of MUFA and PUFAs (Winston et al., 1996).

4.3. Comparison of hemocyte and plasma metabolomics profiles

Our analysis showed an 85 % similarity in the metabolite composition of hemocyte extracts and plasma samples, but the plasma was richer and more concentrated in metabolites than the hemocyte extracts, as previously reported (Frizzo et al., 2021). Osmolytes (taurine, hypotaurine, betaine, Gly, Ala) had the highest signal intensity in both matrices, highlighting the importance of osmoconformity in mussel physiology, with amino acids being the most abundant compounds. The major difference between matrices was the presence of carboxylic acid salts (pyruvate, malate, malonate, galactarate), nucleotides (UMP, GMP), and tyramine in the hemocyte extracts, and the absence of glycolate, and 4-guanidinobutanoate (gamma amino acids). Pyruvate and malate are markers of energy metabolism in the cells, as pyruvate is the final product of glycolysis, and malate is involved in the Krebs cycle for the production of ATP. We cannot rule out that the glycolate circulating in the plasma could originate from algae in the mussel diet, because unicellular green algae can produce glycolate by photorespiration *via* oxygenation of ribulose-1,5-bisphosphate, usually during suboptimal growth periods at high temperatures (Taubert et al., 2019; Bruin et al., 1970). Only two molecules specific to molluscs were identified in the metabolomes: mytilitol (a cyclohexanol) and homarine (a pyridinecarboxylic acid) (Aru et al., 2020; Tikunov et al., 2010; Netherton and Gurin, 1982). Trigonelline, an alkaloid product of the metabolism of niacin (vitamin B3), detected in vegetables and cereals, was putatively identified in both matrices. NMR signals similar to those for this metabolite have been detected in another study of mussels, but the presence of trigonelline in mussels has never been ascertained (Frizzo et al., 2021). This clearly illustrates the lack of knowledge of NMR signatures of metabolites specific to marine organisms and explains why almost 20 % of the signals detected in the NMR spectra of the hemocytes and plasma could not be identified.

Nevertheless, this first attempt at establishing the effect of HAB on mussel hemocytes and general metabolomes showed changes in 47 % and 44 % of the metabolites identified in the hemocytes and plasma, respectively.

4.3.1. A. catenella affects the energy metabolism of the hemocytes

The effect of *A. catenella* upon the energy metabolism of the hemocytes was revealed by changes in several reporting molecules. The explicative and predictive OPLS-DA model based upon hemocyte data highlighted a higher level of carbohydrates (glucose, maltose) and ATP in the control. However, AMP and ADP were higher in STX-exposed mussels, indicating a modification of the energy balance in the hemocytes. The feeding of mussels exposed to the toxic dinoflagellate may also have been altered (discussed below), thus reducing the general production of ATP. Hemocytes may also use more energy to eliminate the algal toxins or to trigger ROS response (Cruz et al., 2007). The acetylcarnitine product of the reaction to produce the co-enzyme A (CoA) from acetyl-CoA and carnitine was higher in the control hemocytes, which may be another indicator of a higher production of ATP in this group, as CoA is involved in the Krebs cycle.

UDP – a ribonucleoside diphosphate sometimes associated with

glucose and involved in glycogenesis – was also higher in the control hemocytes. Indeed, before glucose can be stored as glycogen in granules (abundant in mussel granulocytes (Cajaraville and Pal, 1995)), the enzyme glycogen synthase combines UDP-glucose units to form a glycogen chain (Koyama et al., 2020; Gabbott and Whittle, 1986). The higher level of UDP/UDP-glucose in the control is consistent with a higher energetic status, as well as the higher content of carbohydrates, and may imply a higher ability to synthesize and store glycogen as energy storage. The related compounds uracil and UMP were also higher in the control group. Conversely, STX-exposed hemocytes may have lower glycogen storage and less energy since AMP and ADP (the products of ATP hydrolysis in cells) were higher. Glycogen could not be quantified as it was not extracted during sample preparation.

Two disruptors of mitochondrial functions, malonate and formate, were higher in the hemocytes of mussels exposed to *A. catenella*. Malonate can cause rapid mitochondrial potential collapse and ROS production that overwhelms the mitochondria's antioxidant capacity and leads to cell swelling (Fernandez-Gomez et al., 2005). Formate is a byproduct of acetate production and is responsible for the disruption of mitochondrial electron transport and energy production by inhibiting cytochrome oxidase activity, the terminal electron acceptor of the electron transport chain. This mechanism can lead to cell death from depletion of ATP and increased production of cytotoxic ROS secondary to the blockade of the electron transport chain. Malonate and formate might be molecular precursors of the increased production of ROS by hemocyte mitochondria as a defense mechanism (Donaghy et al., 2012). They may also lead to hemocyte mortality when exposed to higher doses of STX, but not at such a low STX dose as achieved in the present study.

Bivalve cells rely upon free amino acids (FAA) to produce energy by oxidation or gluconeogenesis (Ponder et al., 2019). Our results do not, however, show a preference for this mode of energy production in the hemocytes. Indeed, some glucogenic amino acids were more present in the cytoplasm of the hemocytes exposed to *A. catenella* (Arg, Asp, Gly, Ile, Phe, sarcosine) and others (Ala, Ser, Trp) in the control group. The presence of FAAs also have another function: the regulation of isosmotic cell volume, as will be discussed below.

4.3.2. *A. catenella affects hemocyte osmolyte composition and anti-oxidant profile*

To maintain normal cell and hemocyte-specific functions, organisms more primitive than crustaceans compensate for the salinity level in their environment by changing FAA concentrations. Aminopeptidase-I plays a critical role in creating this pool of amino acids that maintains the isoconformity in the cells, by breaking down proteins and polypeptides into FAAs at the lysosomal level (Hilbish and Koehn, 1987). In mussels, the major osmolytes are Gly, Ala and its isomer β-Ala, taurine and their derivatives dimethylglycine, betaine (trimethylglycine) and hypotaurine. Homarine is derived from Gly and is specific to marine organisms. It is involved in methylation reactions to create betaine, and may also function as an osmolyte (May et al., 2017; Kube et al., 2007; Yancey, 2005), as does dimethylamine (Zhang et al., 2011).

Ala, β-Ala and taurine were higher in the hemocytes of the control group; whereas, Gly and dimethylglycine were lower as compared to the STX-exposed mussels. Other studies have reported that an increased concentration of β-Ala enhances carbohydrate metabolism in mussels (Wang et al., 2021), and is a taurine transport inhibitor (Jong et al., 2012). In addition, taurine has antioxidant properties, protecting the mitochondria against excessive superoxide generation (Jong et al., 2012). Thus, the lower level of the anti-oxidant taurine in the hemocytes following the toxic treatment could help maintain production of ROS by mitochondria as part of the immune response (Winston et al., 1996).

Interestingly, only Ala varied in the same way as in the OPLS-DA adjusted to the plasma metabolites. Hypotaurine, Ala and dimethylglycine were higher in the plasma of the controls, but betaine, taurine, and homarine were higher in the plasma following toxic treatment. The higher contents of betaine and taurine – two antioxidants – in the exposed mussels may have a protective effect against ROS (Liang et al., 2020; Zhang et al., 2016). Mussels exposed to toxins tended to produce more ROS, which induced an antioxidant and detoxifying response involving enzymes such as superoxide dismutase or glutathione-S-transferase, but also molecules such as glutathione (Liu et al., 2020) or betaine and taurine.

4.3.3. *A. catenella seems to affect food intake*

The OPLS-DA model showed lower carbohydrates (maltose, glucose), but also UDP/UDP-glucose and uracil (see above) circulating in the plasma of mussels exposed to the toxic dinoflagellate, suggesting that mussels may stop or reduce feeding as reported in juvenile oysters (Cassis, 2005). The behavioral response of oysters when exposed to toxigenic *Alexandrium* spp., which also produce STX, is complete closure and feeding cessation. In *M. edulis* mussels, the response is different. At intermediary algal densities, similar to that archived in our experimental conditions, increased valve opening could be explained by a paralysis of the adductor muscle, potentially interfering with the control of the filtration process (Durier et al., 2022). Glycolate – a molecule that could originate from the algae in the diet – as well as all the amino acids present in the model based upon the plasma [Arg, Asp, Gln, Glu, Phe, Ser, Trp, Tyr, ornithine (a precursor of Arg), and 2-aminobutyrate (Ile-biosynthesis)], were also in lower levels in mussels exposed to the toxic treatment, which could be another indicator of lower feed intake. Moreover, the higher level of ATP-hydrolysis products (ADP, AMP) in the plasma may be indicative of lower energy following feeding cessation exacerbated by the higher need for energy to reject the toxic dinoflagellates and eliminate toxins that made it inside the organism.

5. Conclusion

This work intended to study the effect of a HAB upon blue mussel immune response. A 120 h exposure of blue mussels to *A. catenella* led to moderate STX contamination of the tissues, with an average concentration of 26 (23) μg STX/100 g of mussel soft tissues. At this sub-lethal toxin concentration (Bricelj et al., 2005), several effects upon hemocyte activity were detected. The aggregated changes are consistent with activation of defense mechanisms in granular hemocytes and a stress response in agranular cells, both consuming energy and changing the overall metabolic status of the mussels.

The implementation of ^{1}H NMR-based metabolomics as a high-throughput profiling and classification tool opens new perspectives to understand the effects of HAB upon mussel general and immune metabolisms. This study offers a new approach to decipher biochemical pathways in mussels, involving hemocyte activity measurement, lipid composition determination, and the first NMR-detected metabolomic investigation of hemocytes and their plasma.

Author contributions

S.B. drafted the manuscript, performed the NMR-based metabolomics, chemometrics, and biological integration. O.G. carried out the index measurements and lipid composition analysis under the supervision of R.T. as well as the cytometry analyzes under the supervision of G. H.W. B.G. established the SXT dosage method and performed the analyses. A.A.A. and D.E.W. contributed to the development of the NMR experiments applied to mussel hemocytes. R.T. and I.M. designed and supervised the study. S.B., A.A.A., D.E.W, G.H.W., R.T., and I. M. contributed to write the manuscript. All authors have approved the final article.

Funding

This project was supported by Environment and Climate Change Canada (FDE-CA-2017i002 to R.T.), the Natural Sciences and Engineering Research Council (NSERC) of Canada (grant RGPIN-

2018–06200 to I.M.) and the Ressources Aquatiques Québec research network (Fonds de Recherche du Québec – Nature et Technologies, no. 2014-RS-171172). Fisheries and Oceans Canada provided in-kind assistance motivated by the Galway Statement on Atlantic Ocean Cooperation.

Declaration of Competing Interest

The authors have no known competing financial interests or personal relationships that could have appeared to influence the work reported in this paper.

Data availability

Data will be made available on request.

Acknowledgements

The authors wish to thank Nathalie Gauthier and Jean-Bruno Nadalini for technical support and Tiago Hori from Atlantic Aqua Farms to supply mussels. Pr. Lekha Sleno as well as Leanne Ohlund (UQAM) are acknowledged for laboratory access and technical support. All authors are members of Ressources Aquatiques Québec.

Supplementary materials

Supplementary material associated with this article can be found, in the online version, at doi:10.1016/j.hal.2023.102529.

References

Abi-Khalil, C., Finkelstein, D.S., Conejero, G., du Bois, J., Destoumieux-Garzon, D., Rolland, J.L., 2017. The paralytic shellfish toxin, saxitoxin, enters the cytoplasm and induces apoptosis of oyster immune cells through a caspase-dependent pathway. Aquat. Toxicol. 190, 133–141. https://doi.org/10.1016/j.aquatox.2017.07.001.

Andreyeva, A.Y., Efremova, E.S., Kukhareva, T.A., 2019. Morphological and functional characterization of hemocytes in cultivated mussel (Mytilus galloprovincialis) and effect of hypoxia on hemocyte parameters. Fish Shellfish Immunol. 89, 361–367. https://doi.org/10.1016/j.fsi.2019.04.017.

Aru, V., Motawie, M.S., Khakimov, B., Sørensen, K.M., Møller, B.L., Engelsen, S.B., 2020. First-principles identification of C-methyl-scyllo-inositol (mytilitol) - A new species-specific metabolite indicator of geographic origin for marine bivalve molluscs (Mytilus and Ruditapes spp. Food Chem. 328, 126959 https://doi.org/10.1016/j.foodchem.2020.126959.

Bates, S.S., Beach, D.G., Comeau, L.A., Haigh, N., Lewis, N.I., Locke, A., Martin, J.L., Mccarron, P., Mckenzie, C.H., Michel, C., Miles, C.O., Poulin, M., Quilliam, M.A., Rourke, W.A., Scarratt, M.G., Starr, M., Wells, T., 2020. Marine harmful algal blooms and phycotoxins of concern to Canada Canadian Technical Report of Fisheries and Aquatic Sciences 3384. Can. Tech. Rep. Fish. Aquat. Sci. 3384.

Bayona, L.M., de Voogd, N.J., Choi, Y.H., 2022. Metabolomics on the study of marine organisms. Metabolomics 18, 17. https://doi.org/10.1007/s11306-022-01874-y.

Beauclercq, S., Mignon-Grasteau, S., Petit, A., Berger, Q., Lefèvre, A., Métayer-Coustard, S., Tesseraud, S., Emond, P., Berri, C., Le Bihan-Duval, E., 2022. A divergent selection on breast meat ultimate pH, a key factor for chicken meat quality, is associated with different circulating lipid profiles. Front. Physiol. 13 https://doi.org/10.3389/fphys.2022.935868.

Beauclercq, S., Nadal-Desbarats, L., Hennequet-Antier, C., Collin, A., Tesseraud, S., Bourin, M., Le Bihan-Duval, E., Berri, C., 2016. Serum and muscle metabolomics for the prediction of ultimate pH, a key factor for chicken-meat quality. J. Proteome. Res. 15, 1168–1178. https://doi.org/10.1021/acs.jproteome.5b01050.

Bianchi, V.A., Bickmeyer, U., Tillmann, U., Krock, B., Müller, A., Abele, D., 2021. In vitro effects of paralytic shellfish toxins and lytic extracellular compounds produced by alexandrium strains on hemocyte integrity and function in Mytilus edulis. Toxins (Basel) 13. https://doi.org/10.3390/toxins13080544.

Bianchi, V.A., Langeloh, H., Tillmann, U., Krock, B., Müller, A., Bickmeyer, U., Abele, D., 2019. Separate and combined effects of neurotoxic and lytic compounds of Alexandrium strains on Mytilus edulis feeding activity and hemocyte function. Fish Shellfish Immunol. 84, 414–422. https://doi.org/10.1016/j.fsi.2018.10.024.

Blasco, D., Levasseur, M., Bonneau, E., Gelinas, R., Packard, T.T., 2003. Patterns of paralytic shellfish toxicity in the St. Lawrence region in relationship with the abundance and distribution of Alexandrium tamarense. Sci. Mar. 67, 261–278.

Boivin-Rioux, A., Starr, M., Chassé, J., Scarratt, M., Perrie, W., Long, Z., 2021. Predicting the effects of climate change on the occurrence of the toxic dinoflagellate alexandrium catenella along Canada's east coast. Front. Mar. Sci.

Bricelj, V.M., Connell, L., Konoki, K., MacQuarrie, S.P., Scheuer, T., Catterall, W.A., Trainer, V.L., 2005. Sodium channel mutation leading to saxitoxin resistance in clams increases risk of PSP. Nature 434, 763–767. https://doi.org/10.1038/nature03415.

Bruin, W.J., Nelson, E.B., Tolbert, N.E., 1970. Glycolate pathway in green algae. Plant Physiol. 46, 386–391. https://doi.org/10.1104/pp.46.3.386.

Cajaraville, M.P., Pal, S.G., 1995. Morphofunctional study of the haemocytes of the bivalve mollusc Mytilus galloprovincialis with emphasis on the endolysosomal compartment. Cell Struct. Funct. 20, 355–367. https://doi.org/10.1247/CSF.20.355.

Campos, A., Apraiz, I., da Fonseca, R.R., Cristobal, S., 2015. Shotgun analysis of the marine mussel Mytilus edulis hemolymph proteome and mapping the innate immunity elements. Proteomics 15, 4021–4029. https://doi.org/10.1002/pmic.201500118.

Cantrell, C.B., Mohiuddin, S.S., 2022. Biochemistry, ketone metabolism. StatPearls. StatPearls Publishing LLC., Treasure IslandFL.

Cassis, D., 2005. The Effect of Harmful Algae On the Summer Mortality of Juvenile Pacific Oysters (Crassostrea Gigas). The University of British Columbia, Vancouver.

Cheng 1, T.C., 1996. Haemocytes: forms and functions. In: Kennedy, V., Newell, R., Eble, A. (Eds.), The Eastern Oyster Crassostrea Virginica. Maryland Sea Grant, College Park, pp. 299–333.

Comeau, L.A., Babarro, J.M.F., Riobó, P., Scarratt, M., Starr, M., Tremblay, R., 2019. PSP-producing dinoflagellate Alexandrium minutum induces valve microclosures in the mussel Mytilus galloprovincialis. Aquaculture 500, 407–413. https://doi.org/10.1016/j.aquaculture.2018.10.025.

Cruz, C.M., Rinna, A., Forman, H.J., Ventura, A.L.M., Persechini, P.M., Ojcius, D.M., 2007. ATP activates a reactive oxygen species-dependent oxidative stress response and secretion of proinflammatory cytokines in macrophages. J. Biol. Chem. 282, 2871–2879. https://doi.org/10.1074/JBC.M608083200.

Cusick, K.D., Sayler, G.S., 2013. An overview on the marine neurotoxin, saxitoxin: genetics, molecular targets, methods of detection and ecological functions. Mar. Drugs 11, 991–1018.

de la Ballina, N.R., Maresca, F., Cao, A., Villalba, A., 2022. Bivalve haemocyte subpopulations: a review. Front. Immunol. 13, 826255 https://doi.org/10.3389/fimmu.2022.826255.

Delaporte, M., Soudant, P., Moal, J., Giudicelli, E., Lambert, C., Seguineau, C., Samain, J. F., 2006. Impact of 20 : 4n-6 supplementation on the fatty acid composition and hemocyte parameters of the Pacific oyster Crassostrea gigas. Lipids 41, 567–576.

Digilio, G., Sforzini, S., Cassino, C., Robotti, E., Oliveri, C., Marengo, E., Musso, D., Osella, D., Viarengo, A., 2016. Haemolymph from Mytilus galloprovincialis: response to copper and temperature challenges studied by 1H-NMR metabonomics. Compar. Biochem. Physiol. Part C Toxicol. Pharmacol. 183–184, 61–71. https://doi.org/10.1016/J.CBPC.2016.02.003.

Donaghy, L., Kraffe, E., Goïc, N., Lambert, C., Volety, A.K., Soudant, P., 2012. Reactive oxygen species in unstimulated hemocytes of the Pacific oyster Crassostrea gigas: a mitochondrial involvement. PLoS ONE 7. https://doi.org/10.1371/journal.pone.0046594.

Durier, G., Nadalini, J.B., Comeau, L.A., Starr, M., Michaud, S., Tran, D., St-Louis, R., Babarro, J.M.F., Clements, J.C., Tremblay, R., 2022. Use of valvometry as an alert tool to signal the presence of toxic algae Alexandrium catenella by Mytilus edulis. Front. Mar. Sci. 9, 1930. https://doi.org/10.3389/FMARS.2022.987872/BIBTEX.

FAO, 2020. The state of world fisheries and aquaculture 2020. Sustainability in Action. Rome. https://doi.org/10.4060/ca9229en.

Fernandez-Gomez, F.J., Galindo, M.F., Gómez-Lázaro, M., Yuste, V.J., Comella, J.X., Aguirre, N., Jordán, J., 2005. Malonate induces cell death via mitochondrial potential collapse and delayed swelling through an ROS-dependent pathway. Br. J. Pharmacol. 144, 528. https://doi.org/10.1038/SJ.BJP.0706069.

Frizzo, R., Bortoletto, E., Riello, T., Leanza, L., Schievano, E., Venier, P., Mammi, S., 2021. NMR metabolite profiles of the bivalve mollusc mytilus galloprovincialis before and after immune stimulation with vibrio splendidus. Front. Mol. Biosci. 8, 731. https://doi.org/10.3389/FMOLB.2021.686770/BIBTEX.

Gabbott, P.A., Whittle, M.A., 1986. Glycogen synthetase in the sea mussel Mytilus edulis L.—II. Seasonal changes in glycogen content and glycogen synthetase activity in the mantle tissue. Compar. Biochem. Physiol. Part B Compar. Biochem. 83, 197–207. https://doi.org/10.1016/0305-0491(86)90353-6.

Galimany, E., Sunila, I., Hegaret, H., Ramon, M., Wikfors, G.H., 2008a. Pathology and immune response of the blue mussel (Mytilus edulis L.) after an exposure to the harmful dinoflagellate Prorocentrum minimum. Harmful Algae 7, 630–638. https://doi.org/10.1016/j.hal.2008.01.001.

Galimany, E., Sunila, I., Hégaret, H., Ramón, M., Wikfors, G.H., 2008b. Experimental exposure of the blue mussel (Mytilus edulis, L.) to the toxic dinoflagellate Alexandrium fundyense: histopathology, immune responses, and recovery. Harmful Algae 7, 702–711. https://doi.org/10.1016/j.hal.2008.02.006.

Gosling, E., 2008. Bivalve molluscs: biology, Ecology and Culture. John Wiley & Sons.

Hegaret, H., Wikfors, G.H., Shumway, S.E., 2007. Diverse feeding responses of five species of bivalve mollusc when exposed to three species of harmful algae. J. Shellfish Res. 26, 549–559.

Hegaret, H., Wikfors, G.H., Soudant, P., 2003. Flow-cytometric analysis of haemocytes from eastern oysters, Crassostrea virginica, subjected to a sudden temperature elevation: I. Haemocyte types and morphology. J. Exp. Mar. Biol. Ecol 293, 237–248.

Hilbish, T.J., Koehn, R.K., 1987. The adaptive importance of genetic variation. Am. Sci. 75, 134–141.

Jacob, D., Deborde, C., Lefebvre, M., Maucourt, M., Moing, A., 2017. NMRProcFlow: a graphical and interactive tool dedicated to 1D spectra processing for NMR-based metabolomics. Metabolomics 13, 36. https://doi.org/10.1007/s11306-017-1178-y.

John, U., Litaker, W., Montresor, M., Murray, S., Brosnahan, M.L., Anderson, D.M., 2014. 2302) Proposal to reject the name Gonyaulax catenella (Alexandrium catenella) (Dinophyceae). Taxon 63, 932. https://doi.org/10.12705/634.21.

Jong, C.J., Azuma, J., Schaffer, S., 2012. Mechanism underlying the antioxidant activity of taurine: prevention of mitochondrial oxidant production. Amino Acids 42, 2223–2232. https://doi.org/10.1007/s00726-011-0962-7.

Koyama, M., Furukawa, F., Koga, Y., Funayama, S., Furukawa, S., Baba, O., Lin, C.C., Hwang, P.P., Moriyama, S., Okumura, S.I., 2020. Gluconeogenesis and glycogen metabolism during development of Pacific abalone, Haliotis discus hannai. Am. J. Physiol. Regul. Integr. Comp. Physiol. 318, R619–R633. https://doi.org/10.1152/AJPREGU.00211.2019/ASSET/IMAGES/LARGE/ZH60032098310008.JPEG.

Kube, S., Sokolowski, A., Jansen, J.M., Schiedek, D., 2007. Seasonal variability of free amino acids in two marine bivalves, Macoma balthica and Mytilus spp., in relation to environmental and physiological factors. Comp. Biochem. Physiol. A Mol. Integr. Physiol. 147, 1015–1027. https://doi.org/10.1016/J.CBPA.2007.03.012.

Lassudrie, M., Hégaret, H., Wikfors, G.H., da Silva, P.M., 2020. Effects of marine harmful algal blooms on bivalve cellular immunity and infectious diseases: a review. Dev. Comp. Immunol. 108, 103660.

Lavaud, R., Durier, G., Nadalini, J.-B., Filgueira, R., Comeau, L.A., Babarro, J.M.F., Michaud, S., Scarratt, M., Tremblay, R., 2021. Effects of the toxic dinoflagellate Alexandrium catenella on the behaviour and physiology of the blue mussel Mytilus edulis. Harmful Algae 108, 102097. https://doi.org/10.1016/j.hal.2021.102097.

le Grand, F., Kraffe, E., Marty, Y., Donaghy, L., Soudant, P., 2011. Membrane phospholipids compositions of hemocytes in the Pacidic oyster Crassostrea gigas and the Manila clam Ruditapes philippinarum. Comp. Biochem. Physiol. 159A, 383–391.

le Grand, F., Soudant, P., Marty, Y., le Goïc, N., Kraffe, E., 2013. Altered membrane lipid composition and functional parameters of circulating cells in cockles (Cerastoderma edule) affected by disseminated neoplasia. Chem. Phys. Lipids 167–168, 9–20.

le Grand, F., Soudant, P., Siah, A., Tremblay, R., Marty, Y., Kraffe, E., 2014. Disseminated neoplasia in the soft-shell clam Mya arenaria: membrane lipid composition and functional parameters of circulating cells. Lipids 49, 807–818.

Leroux, N., Hosseinzadeh, M., Katsumiti, A., Porte, C., Cajaraville, M.P., 2022. Lipidomic analysis of mussel hemocytes exposed to polystyrene nanoplastics. Environ. Res. 214, 113763 https://doi.org/10.1016/j.envres.2022.113763.

Liang, R., Shao, X., Shi, Y., Jiang, L., Han, G., 2020. Antioxidant defenses and metabolic responses of blue mussels (Mytilus edulis) exposed to various concentrations of erythromycin. Sci. Total Environ. 698, 134221 https://doi.org/10.1016/J.SCITOTENV.2019.134221.

Liu, Y., Li, L., Zheng, L., Fu, P., Wang, Y., Nguyen, H., Shen, X., Sui, Y., 2020. Antioxidant responses of triangle sail mussel Hyriopsis cumingii exposed to harmful algae Microcystis aeruginosa and high pH. Chemosphere 243, 125241. https://doi.org/10.1016/J.CHEMOSPHERE.2019.125241.

Madji Hounoum, B., Blasco, H., Nadal-Desbarats, L., Diémé, B., Montigny, F., Andres, C. R., Emond, P., Mavel, S., 2015. Analytical methodology for metabolomics study of adherent mammalian cells using NMR, GC–MS and LC-HRMS. Anal. Bioanal. Chem. 407, 8861–8872. https://doi.org/10.1007/s00216-015-9047-x.

Marty, Y., Delaunay, F., Moal, J., Samain, J.-F., 1992. Changes in the fatty acid composition of Pecten maximus (L.) during larval development. J. Exp. Mar. Biol. Ecol. 163, 221–234.

May, M.A., Bishop, K.D., Rawson, P.D., 2017. NMR Profiling of metabolites in larval and juvenile blue mussels (mytilus edulis) under ambient and low salinity conditions. Metabolites 7. https://doi.org/10.3390/METABO7030033.

Netherton, J.C., Gurin, S., 1982. Biosynthesis and physiological role of homarine in marine shrimp. J. Biol. Chem. 257, 11971–11975. https://doi.org/10.1016/s0021-9258(18)33662-7.

Nguyen, T.v, Alfaro, A.C., 2020. Applications of omics to investigate responses of bivalve haemocytes to pathogen infections and environmental stress. Aquaculture 518, 734488. https://doi.org/10.1016/j.aquaculture.2019.734488.

Nielsen, L.T., Hansen, P.J., Krock, B., Vismann, B., 2016. Accumulation, transformation and breakdown of DSP toxins from the toxic dinoflagellate Dinophysis acuta in blue mussels, Mytilus edulis. Toxicon 117, 84–93. https://doi.org/10.1016/J.TOXICON.2016.03.021.

Parrish, C., 1987. Separation of aquatic lipid classes by chromarod thin-layer chromatography with measurement by Iatroscan Flame Ionization detection. Can. J. Fish. Aquat. Sci. 44, 722–731.

Parrish, C.C., 1999. Determination of total lipid, lipid classes, and fatty acids in aquatic samples. In: Arts, M.T., Wainman, B.C. (Eds.), Lipids in Freshwater Ecosystems. Springer-Verlag, New York, pp. 4–20.

Ponder, W.F., Lindberg, D.R., Ponder, J.M., 2019. Overview of molluscan physiology and genomics. Biology and Evolution of the Mollusca. Taylor & Francis, Boca Raton.

Pousse, É., Flye-Sainte-Marie, J., Alunno-Bruscia, M., Hégaret, H., Rannou, É., Pecquerie, L., Marques, G.M., Thomas, Y., Castrec, J., Fabioux, C., Long, M., Lassudrie, M., Hermabessiere, L., Amzil, Z., Soudant, P., Jean, F., 2019. Modelling paralytic shellfish toxins (PST) accumulation in Crassostrea gigas by using Dynamic Energy Budgets (DEB). J. Sea Res. 143, 152–164. https://doi.org/10.1016/j.seares.2018.09.002.

Qiu, J., Ji, Y., Fang, Y., Zhao, M., Wang, S., Ai, Q., Li, A., 2020. Response of fatty acids and lipid metabolism enzymes during accumulation, depuration and esterification of diarrhetic shellfish toxins in mussels (Mytilus galloprovincialis). Ecotoxicol. Environ. Saf. 206, 111223 https://doi.org/10.1016/j.ecoenv.2020.111223.

Soudant, P., Paillard, C., Choquet, G., Lambert, C., Reid, H.I., Marhic, A., Donaghy, L., Birkbeck, T.H., 2004. Impact of season and rearing site on the physiological and immunological parameters of the Manila clam Venerupis (=Tapes, =Ruditapes) philippinarum. Aquaculture 229, 401–418.

Starr, M., Lair, S., Michaud, S., Scarratt, M., Quilliam, M., Lefaivre, D., Robert, M., Wotherspoon, A., Michaud, R., Ménard, N., Sauvé, G., Lessard, S., Béland, P., Measures, L., 2017. Multispecies mass mortality of marine fauna linked to a toxic dinoflagellate bloom. PLoS ONE 12, e0176299. https://doi.org/10.1371/journal.pone.0176299.

Statistics-Canada, 2019. Statistique Canada, 2019. Production D'aquaculture En Quantité Et En Valeurs. https://www.dfo-mpo.gc.ca/stats/aqua/aqua19-fra.htm.

Taubert, A., Jakob, T., Wilhelm, C., 2019. Glycolate from microalgae: an efficient carbon source for biotechnological applications. Plant Biotechnol. J. 17, 1538–1546. https://doi.org/10.1111/pbi.13078.

Tikunov, A.P., Johnson, C.B., Lee, H., Stoskopf, M.K., Macdonald, J.M., 2010. Metabolomic investigations of American oysters using H-NMR spectroscopy. Mar. Drugs 8, 2578–2596. https://doi.org/10.3390/md8102578.

Tran, D., Haberkorn, H., Soudant, P., Ciret, P., Massabuau, J.-C., 2010. Behavioral responses of Crassostrea gigas exposed to the harmful algae Alexandrium minutum. Aquaculture 298, 338–345.

Tremblay, R., Landry, T., 2016. The implication of metabolic performance of Mytilus edulis, Mytilus trossulus, and hybrids for mussel aquaculture in eastern canadian waters. J. Mar. Biol. Aquacult. 2, 1–7.

Turrens, J.F., 2003. Mitochondrial formation of reactive oxygen species. J. Physiol. 552, 335–344. https://doi.org/10.1111/j.1469-7793.2003.00335.x.

Wang, C.yue, Yan, X.jun, He, J.yu, Buttino, I., Pan, C., Fan, M.hua, Guo, B.ying, Zhang, X. lin, Liao, Z., 2021. Responses to β-alanine and carnosine supplementation of mussel Mytilus coruscus as revealed by UPLC–MS/MS based untargeted metabolomics. Aquac. Rep. 20, 100730 https://doi.org/10.1016/J.AQREP.2021.100730.

Wang, J., Salata, J.J., Bennett, P.B., 2003. Saxitoxin is a gating modifier of HERG K+ channels. J. Gen. Physiol. 121, 583–598. https://doi.org/10.1085/jgp.200308812.

Wikfors, G.H., Alix, J.H., 2014. Granular hemocytes are phagocytic, but agranular hemocytes are not. In: the Eastern Oyster Crassostrea virginica. Invertebrate Immunity, 1. https://doi.org/10.2478/INVIM-2014-0001.

Winston, G.W., Moore, M.N., Kirchin, M.A., Soverchia, C., 1996. Production of reactive oxygen species by Hemocytes from the marine mussel, Mytilus edulis: lysosomal localization and effect of xenobiotics. Comp. Biochem. Physiol. C Pharmacol. Toxicol. Endocrinol. 113, 221–229. https://doi.org/10.1016/0742-8413(95)02091-8.

Wishart, D.S., Guo, A., Oler, E., Wang, F., Anjum, A., Peters, H., Dizon, R., Sayeeda, Z., Tian, S., Lee, B.L., Berjanskii, M., Mah, R., Yamamoto, M., Jovel, J., Torres-Calzada, C., Hiebert-Giesbrecht, M., Lui, V.W., Varshavi, D., Varshavi, D., Allen, D., Arndt, D., Khetarpal, N., Sivakumaran, A., Harford, K., Sanford, S., Yee, K., Cao, X., Budinski, Z., Liigand, J., Zhang, L., Zheng, J., Mandal, R., Karu, N., Dambrova, M., Schiöth, H.B., Greiner, R., Gautam, V., 2022. HMDB 5.0: the Human Metabolome Database for 2022. Nucleic Acids Res. 50, D622–d631. https://doi.org/10.1093/nar/gkab1062.

Yancey, P.H., 2005. Organic osmolytes as compatible, metabolic and counteracting cytoprotectants in high osmolarity and other stresses. J. Experim. Biol. 208, 2819–2830. https://doi.org/10.1242/JEB.01730.

Young, T., Alfaro, A.C., 2018. Metabolomic strategies for aquaculture research: a primer. Rev. Aquac. 10, 26–56. https://doi.org/10.1111/raq.12146.

Zacharias, H.U., Altenbuchinger, M., Gronwald, W., 2018. Statistical analysis of NMR metabolic fingerprints: established methods and recent advances. Metabolites 8. https://doi.org/10.3390/metabo8030047.

Zhang, L., Liu, X., You, L., Zhou, D., Wu, H., Li, L., Zhao, J., Feng, J., Yu, J., 2011. Metabolic responses in gills of Manila clam Ruditapes philippinarum exposed to copper using NMR-based metabolomics. Mar. Environ. Res. 72, 33–39. https://doi.org/10.1016/J.MARENVRES.2011.04.002.

Zhang, M., Zhang, H., Li, H., Lai, F., Li, X., Tang, Y., Min, T., Wu, H., 2016. Antioxidant mechanism of betaine without free radical scavenging ability. J. Agric. Food Chem. 64, 7921–7930. https://doi.org/10.1021/ACS.JAFC.6B03592/ASSET/IMAGES/LARGE/JF-2016-03592Z_0007.JPEG.

Metabolomics and lipidomics reveal the effects of the toxic dinoflagellate *Alexandrium catenella* on immune cells of the blue mussel, *Mytilus edulis*

Stéphane Beauclercq[a], Olivier Grenier[b], Alexandre A. Arnold[a], Dror E. Warschawski[c], Gary H. Wikfors[d], Bertrand Genard[b,e], Réjean Tremblay[b*], Isabelle Marcotte[a,*]

[a]Department of Chemistry, Université du Québec à Montréal, P.O. Box 8888, Downtown Station, Montréal, QC, Canada

[b]Institut des Sciences de la Mer de Rimouski, Université du Québec à Rimouski, Rimouski, QC, Canada

[c]Laboratoire des Biomolécules, LBM, CNRS UMR 7203, Sorbonne Université, École Normale Supérieure, PSL University, Paris, France

[d]Northeast Fisheries Science Center (NEFSC), NOAA Fisheries, Milford, CT, USA

[e]Les laboratoires Iso-BioKem Inc., 367 rue Gratien-Gélinas, Rimouski, QC, Canada.

Corresponding authors: Isabelle Marcotte (marcotte.isabelle@uqam.ca) and Réjean Tremblay (rejean.tremblay@uqar.ca)

Saxitoxin dosage protocol

- **Extraction**

- Freeze dry the mussel tissues for 24 hours
- Grind the samples and transfer to 5 mL propylene tubes
- Sonicate the samples 5 minutes at room temperature
- Extract with 4 mL 1% acetic acid and vortex 30 min
- Heat the samples in water (95-100°C) for 5 min
- Shake 5 min at room temperature
- Cool down in ice 5 min
- Centrifuge at 2,400×g at room temperature for 5 min
- Recover the supernatants in new tubes
- Repeat the extraction with 4 mL of 1% acetic acid and combine the two fractions
- Adjust the volumes to 10 mL with 1% acetic acid
- Collect 1.5 mL of the crude extracts and place them in microtubes
- Centrifuge at 17,000×g to pellet impurities
- Collect 2 mL of the supernatants and filter (25 mm, 0.2 µm)
- Transfer 100 µL into a new 1.5 mL microtube
- Add 900 µL of 4 mM formate d'ammonium pH 3.5 H2O:ACN (40:60) into the microtube and vortex
- Collect the samples using a 1 mL syringes and filter with a 13 mm, 0.2 µm filter in an HPLC vial
- Keep at 4°C

- **LC-MSMS analysis**

- HPLC parameters:

Column	Poroshell 120, HILIC-Z, 2.1x100mm, 3µm
Column temperature	30°C
Injector temperature	4°C
Flux	500 µL/min
Injection volume	20 µL
Needle wash	5 s Flush Port
Draw speed	200 µl/min
Eject speed	400 µl/min
Run time	10 min
Post time	3 min

- Quaternary pump timetable

Time	**%A (H2O : ACN 40:60)**	**%B (H2O)**
0	100	0
4	100	0
5	0	100
6	100	0
10	100	0

- MS/MS parameters

MS source	ESI
Gas temperature	350°C
Gas flow	13 L/min
Nebulizer	50 psi
Capillary	2,500 V
Polarity	Positive
Scan type	MRM (Multiple reaction monitoring)
Cycle Time	199.5 ms/cycle
Dwell	25
MS1 and MS2 resolution	wide
CAV	7

- MRM parameters from saxitoxin

Precursor Ion	**Product Ion**	**Fragmentor**	**Collision Energy**
300	266	136	12
300	239	136	16
300	221	136	16
300	204	136	24
300	186	136	16
300	138	136	28
300	282	136	16

- **Spectral analysis**

The analysis of the results was done using QQQ quantification software from MassHunter (Agilent Technologies). The method uses the transition 300→138 as the quantizer and transitions 300→204 and 300→282 as the qualifier.

Table S1. Data acquisition parameters for the 2D NMR spectra of hemocyte extracts and plasma

Parameter	COSY	TOCSY
F2 spectral width (ppm)	13	14
F1 spectral width (ppm)	13	14
Size of FID F2	2048	2048
Size of FID F1	514	514
Number of scans (dummy scans)	32 (16)	32 (32)
Relaxation delay (s)	2	1.5
Spin-lock (D9; ms)		60
Pulse sequence	cosygpprqf	dipsi2esgpph

Table S2. Linear regressions between the saxitoxin concentration and the cytometry variables

	R2	**Adusted R^2**	***p***	**Regression slope**
% non-apoptotic living cells	0.02135	-0.03622	0.5506	-0.2365
% non-apoptotic dead cells	0.0002745	-0.05853	0.9463	-0.01669
% apoptotic living cells	0.008305	-0.05003	0.7106	-0.01084
% apoptotic dead cells	0.1217	0.07	0.1433	0.2641
ROS agranular cells (FAU)	0.03229	-0.02463	0.4617	-21.27
ROS granular cells (FAU)	0.05079	-0.005041	0.3535	-861.5